HHS Public Access

Author manuscript

Neuroimage Rep. Author manuscript; available in PMC 2023 March 24.

Published in final edited form as:

Neuroimage Rep. 2021 March ; 1(1): . doi:10.1016/j.ynirp.2021.100005.

Neurite Orientation Dispersion and Density Imaging (NODDI) and Duration of Untreated Psychosis in Antipsychotic Medication-Naïve First Episode Psychosis Patients

Nina Vanessa Kraguljac, MD[1,*], **William Stonewall Monroe**[2], **Thomas Anthony, MSEE**[2], **Ripu Daman Jindal**[3], **Harrison Hill, MD**[1], **Adrienne Carol Lahti, MD**[1]

[1]Department of Psychiatry and Behavioral Neurobiology, University of Alabama at Birmingham

[2]Department of Electrical and Computer Engineering/ IT Research Computing, University of Alabama at Birmingham

[3]Department of Neurology, Birmingham VA Medical Center

Abstract

Background: Diffusion tensor imaging suggests that white matter alterations are already evident in first episode psychosis patients (FEP) and may become more prominent as the duration of untreated psychosis (DUP) increases. But because the tensor model lacks specificity, it remains unclear how to interpret findings on a biological level. Here, we used a biophysical diffusion model, Neurite Orientation Dispersion and Density Imaging (NODDI), to map microarchitecture in FEP, and to investigate associations between DUP and microarchitectural integrity.

Methods: We scanned 78 antipsychotic medication-naïve FEP and 64 healthy controls using a multi-shell diffusion weighted sequence and used the NODDI toolbox to compute neurite density (ND), orientation dispersion index (ODI) and extracellular free water (FW) maps. AFNI's 3dttest++ was used to compare diffusion maps between groups and to perform regression analyses with DUP.

Results: We found that ND was decreased in commissural and association fibers but increased in projection fibers in FEP. ODI was largely increased regardless of fiber type, and FW showed a mix of increase in decrease across fiber tracts. We also demonstrated associations between DUP and microarchitecture for all NODDI indices.

Conclusions: We demonstrated that complex microarchitecture abnormalities are already evident in antipsychotic-naïve FEP. ND alterations are differentially expressed depending on fiber type, while decreased fiber complexity appears to be a uniform marker of white matter deficit in the illness. Importantly, we identified an empirical link between longer DUP and greater white matter pathology across NODDI indices, underscoring the critical importance of early intervention in this devastating illness.

[*]Corresponding Author: Nina Vanessa Kraguljac, MD, Department of Psychiatry and Behavioral Neurobiology, The University of Alabama at Birmingham, SC 501, 1720 7th Ave S, Birmingham, AL 35294-0017, 205-996-7171, nkraguljac@uabmc.edu.

AUTHOR CONTRIBUTIONS

ACL designed and oversaw all aspects of the study. ACL, NVK, HH, and RDJ assisted with subject recruitment and data collection. NVK, WSM and AT developed the data processing pipeline and performed data analysis. NVK wrote the initial draft of the manuscript. All authors contributed to editing of the manuscript and vouch for the integrity of the data.

Keywords

first episode psychosis; white matter; duration of untreated psychosis; free water; neurite density; orientation dispersion

1. INTRODUCTION

Developmental trajectory studies suggest that white matter growth, reflected in an increase in myelination, axonal diameter and change in extracellular space (Brouwer et al., 2012; Lebel and Deoni, 2018), continues to increase well into adulthood (Hasan et al., 2009; Kochunov et al., 2012). Maturation rates are somewhat variable between different white matter tracts, where associative fibers that connect brain regions supporting higher order cognition reach their peak later in life compared to earlier maturing projection fibers such as motor and sensory tracts (Kochunov et al., 2012). Importantly, white matter changes may not only be genetically programmed, but also be subject to environmental influences (Brouwer et al., 2012), and it appears that environmental factors start to outweigh genetics during later adolescence and early adulthood (Chiang et al., 2011).

Schizophrenia is a complex neuropsychiatric syndrome that is characterized by widespread white matter integrity deficits (Kelly et al., 2017) and typically emerges during late adolescence or early adulthood, at a time where white matter continues to undergo maturational processes (Kochunov and Hong, 2014). Diffusion tensor imaging studies have reported widespread white matter deficits in the illness (Kelly et al., 2018); affected pathways include commissural, association and projection fibers. One modifiable environmental factor that may adversely impact white matter maturation in psychosis spectrum disorders is the duration of untreated psychosis (DUP). We recently reported an empirical link between whole brain white matter fractional anisotropy, a tensor-based marker of white matter integrity, and DUP in antipsychotic-naïve first episode psychosis patients (FEP), indicating that white matter alterations become more prominent as the DUP increases (Kraguljac et al., 2020). But because the tensor model lacks specificity, we were unable to determine how DUP impacts white matter integrity on a biological level, whether it affects the volume fraction of neurites (axons and dendrites), fiber complexity, extracellular space, or a combination thereof.

Alternative diffusion models have recently been developed in an effort to overcome these limitations and link the diffusion signal to neuroanatomical microarchitecture (Assaf and Basser, 2005; Fieremans et al., 2011; Zhang et al., 2012). These models are geared towards biophysical characterization of white matter microstructure, potentially providing additional characterization of white matter pathology beyond of what is possible with traditional diffusion tensor models. One method that provides more specific microarchitectural information including neurite density (ND), orientation dispersion (ODI) and extracellular free water (FW) is Neurite Orientation Dispersion and Density Imaging (NODDI). NODDI delineates signal contributions from three tissue compartments (Zhang et al., 2012), where the intra-neurite compartment consists of axons and dendrites, the extra-neurite compartment represents cell bodies and glial cells, and the non-tissue

compartment embodies cerebrospinal fluid. Histological validation studies of NODDI (Colgan et al., 2016; Grussu et al., 2017; Sato et al., 2017; Schilling et al., 2018) have provided unequivocal evidence that the ODI, which assesses the variability of neurite orientation, matches its histological counterpart (Grussu et al., 2017). Unfortunately, it is not feasible to histologically confirm FW as a proxy of inflammation. However, because neuroinflammation increases the volume of water in the extracellular space (Sykova and Nicholson, 2008) it stands to reason that this would be reflected by a corresponding increase of FW. This was empirically supported in a transgenic Alzheimer model which found that the evolution of FW changes corresponds to the inflammatory burden in TgF344-AD rats (Fick et al., 2017). Taken together, NODDI imaging could potentially provide novel insights in the pathophysiological processes that underlie white matter alterations. Importantly, NODDI has also been shown to be more sensitive to microstructural changes in late childhood and adolescence than fractional anisotropy (Genc et al., 2017; Mah et al., 2017), suggesting that these advanced parameters may be more sensitive to detect subtle white matter changes than traditional diffusion tensor imaging.

To expand upon our recent findings (Kraguljac et al., 2020), we applied the NODDI model to our multi-shell diffusion dataset to map the neuroanatomical microarchitecture in antipsychotic-naïve FEP. The goal of this study was twofold. First, we aimed to contrast microarchitectural information between groups. Because of the heterogeneity in developmental trajectories and anatomical makeup of projection fibers (large axon calibers, thickly myelinated) and association fibers (densely packed, thinly myelinated), and because white matter changes in schizophrenia involve dynamic interactions between neuropathological processes in a tract-specific manner (Cetin-Karayumak et al., 2019), we hypothesized that fiber tracts would not express a uniform pattern of microarchitectural alterations. Second, we sought to investigate if DUP is associated with microarchitectural integrity. We hypothesized that longer DUP would be associated with greater white matter architectural alterations in FEP. In an exploratory fashion, we also examined relationships between white matter microarchitecture and disease severity across symptom dimensions, including cognition, positive and negative symptom severity.

2. MATERIALS AND METHODS

2.1. Participants

FEP were recruited from outpatient, inpatient and emergency room settings at the University of Alabama at Birmingham (UAB). Written informed consent was obtained (after being deemed to have capacity to give consent (Carpenter et al., 2000)) prior to enrollment in this UAB Institutional Review Board approved study.

Participants were excluded if they had major neurological or medical conditions, history of head trauma with loss of consciousness, substance use disorders (excluding nicotine and cannabis) within one month of imaging, were pregnant or breastfeeding, or had MRI contraindications. Patients were either antipsychotic-naïve or had no more than five days of lifetime antipsychotic exposure prior to study entry (82.1% of had no prior exposure). Controls with a personal history of a mental illness or family history in a first-degree relative of a psychotic disorder were excluded.

Diagnoses were established by consensus of two board certified psychiatrists (ACL and NVK) taking into consideration information from the Diagnostic Interview for Genetic Studies (DIGS) or Mini-International Neuropsychiatric Interview (MINI) and medical records as available. In addition, because of the longitudinal design of the study (ClinicalTrials.gov Identifier: NCT02034253, NCT03442101) clinical observations over several months of follow up were used to establish a final diagnosis. The Brief Psychiatric Rating Scale (BPRS) and Repeatable Battery for the Assessment of Neuropsychological Status (RBANS) were used to assess symptom severity and cognition, respectively. We operationally defined DUP as the time between first onset of positive symptoms and the start of treatment (the time at which the first antipsychotic prescription was written, which also coincided with enrollment in the study). The time of symptom onset was determined in consensus by two psychiatrists (ACL and NVK) via clinical interviews with the patient and family members as well as medical records (psychiatric assessment, review of systems, family history, laboratory workup) and clinical observations and assessments over several months of follow up.

The dataset here has no subject overlap with our previous NODDI study in psychosis spectrum patients (Kraguljac et al., 2019), but has subject overlap with a recent tensor based study (Kraguljac et al., 2020).

2.2. Data acquisition

All imaging was performed on a 3T Siemens Magnetom Prisma scanner equipped with a 20-channel head coil. A T2 weighted scan was acquired for anatomical reference (TR/TE: 3200/ 563ms; GRAPPA factor 2; slice thickness 0.8mm; 208 slices, voxel size 0.8mm^3).

DWI data was acquired with opposing phase encoding directions (anterior > posterior, and posterior > anterior; [TR/TE: 3230ms/ 89.20ms; multiband acceleration factor 4, Flip angle: 84°; slice thickness 1.5mm, 92 slices, voxel size 1.5mm^3, 92 diffusion weighted images distributed equally over 2 shells with b-values of ~ 1500s/mm^2 and ~ 3000s/mm^2, as well as 7 interspersed b= ~ 0s/mm^2 images for each phase encoding direction]), scan time of 5 minutes 37 seconds for each phase encoding direction.

2.3. Data preprocessing

Preprocessing of DWI images was performed in TORTOISE (version 3.1.2) (Irfanoglu et al., 2017; Pierpaoli et al., 2010). This included correction for thermal noise (Veraart et al., 2016), Gibbs-ringing (Kellner et al., 2016), high b-value based bulk motion and eddy-current distortions using a MAP-MRI model (Ozarslan et al., 2013; Rohde et al., 2004), resampling of images to 1mm^3, and rotation of gradient tables independently for each DWI phase encoding direction using DIFF-PREP. Then, DR-BUDDI was used to correct EPI distortions incorporating information from the undistorted T2 weighted anatomical image combining the two diffusion datasets acquired in opposing phase encoding directions using geometric averaging to generate the corrected dataset (Irfanoglu et al., 2015). For calculation of ND, ODI and FW maps (Figure 1), we used the NODDI toolbox (version 1.0.1) (Zhang et al., 2012). To spatially normalize images to the Illinois Institute of Technology atlas (IIT4)

space, we implemented an optimized non-linear image registration procedure with a mutual information algorithm using a modified version of 3dQwarp in AFNI (Yin et al., 2016).

2.4. Data quality control

We initially verified protocol adherence and visually inspected raw images for signal loss and presence of artifacts. We then assessed bulk motion and excluded datasets with an average root mean square of absolute displacement (RMS_{abs}) of greater than the voxel edge length (1.5mm) or root mean square of relative displacement (RMS_{rel}) of >0.05mm averaged across phase encoding directions from further analyses. DR_BUDDI outputs were assessed for quality of motion, eddy current and EPI distortion correction, and NODDI diffusion maps were inspected for anomalies in parameters.

2.5. Statistical analyses

To examine voxel-wise group differences in ND, ODI and FW between FEP and controls we used AFNI's 3dttest++; co-variates included age, gender, RMS_{rel}, and scan update. Clustsim, a randomization/ permutation simulation to produce 10,000 iterations of noise only generated t-tests and determine global cluster-level threshold values, was implemented to control for the false positive rate (voxelwise threshold Bonferroni corrected p= 0.003 [accounting for 3 comparisons at $p_{uncorrected}$= 0.01]; cluster threshold α= 0.05) (Cox et al., 2017).

We then used regression analyses to examine relationships between whole brain voxel-wise ND, ODI and FW and RBANS, BPRS total, BPRS positive and BPRS negative symptoms scores, as well as log transformed DUP with 3dttest++, using the same covariates as described above. Clustsim was implemented to control for the false positive rate (voxelwise threshold Bonferroni corrected p= 0.00066 [accounting for 15 comparisons at $p_{uncorrected}$= 0.01]; cluster threshold α= 0.05).

3. RESULTS

3.1. Participant characteristics

Of the 212 patients assessed for eligibility between June 2016 and November 2019, 87 FEP were consented and 78 had imaging data obtained (Figure 2). We also enrolled 64 HC. Groups did not differ in gender, age or parental socioeconomic status (Table). Scans for 4 HC and 13 FEP did not pass data quality control and were excluded from statistical analyses.

3.2. Group differences in NODDI indices

NODDI maps detected significant white matter microstructural abnormalities in medication-naïve FEP across commissural, association and projection fibers (Figure 3).

ND was lower in FEP compared to HC in commissural and association fibers including the forceps minor, inferior fronto-occipital fasciculus, inferior longitudinal fasciculus, arcuarte fasciculus and external capsule. ND was higher in FEP compared to HC in the anterior thalamic radiation, which is part of the projection fibers.

ODI was increased in FEP compared to HC across all fiber types including the corpus callosum/ forceps minor, fornix, inferior fronto-occipital fasciculus, uncinate fasciculus, internal and external capsules, the corticospinal tract and cerebral peduncle.

FW in the anterior thalamic radiation and anterior corona radiata was elevated in FEP compared to HC, while FW was decreased in the inferior longitudinal fasciculus, corticospinal tract and posterior thalamic radiation.

3.3. Relationship between NODDI indices and clinical variables

We found associations between DUP and white matter microarchitecture across all three NODDI indices.

Regression analyses showed that greater DUP was associated with lower ND in the commissural fibers including the forceps minor and fornix, as well as association fibers including the arcuate fasciculus, cingulum bundle, and external capsule. The same relationship was found internal capsule. Greater DUP was associated with higher ND in the anterior thalamic radiation, a projection fiber. ND in the superior longitudinal fasciculus showed a mix of positive and negative associations with DUP.

Greater DUP was also associated with higher ODI across fiber types including the corpus callosum and fornix, the arcuate fasciculus, cingulum bundle, and inferior fronto-occipital fasciculus, as well as the internal capsule.

Greater DUP was associated with higher FW in the anterior thalamic radiation and superior longitudinal fasciculus and with lower FW in the fornix, inferior longitudinal fasciculus, inferior fronto-occipital fasciculus, internal and external capsules.

We did not detect associations between ND, ODI or FW and disease severity across symptom dimensions (RBANS total score, BPRS total, positive symptom, and negative symptom score).

4. DISCUSSION

Here, we applied a NODDI model to map, for the first time, the neuroanatomical microarchitecture *in vivo* in antipsychotic-naïve FEP and to investigate the impact of DUP on microarchitectural integrity. We found that ND was decreased in commissural and association fibers, which support higher order cognition, but increased in the earlier maturing projection fibers in FEP. On the other hand, ODI was largely increased regardless of fiber type, and FW showed a mix of increase in decrease across various fiber tracts. We further demonstrated associations between DUP and microarchitecture for all three indices, adding to the emerging experimental evidence consistent with the idea that the DUP may have fundamental pathogenic effects on the brain.

Our finding of decreased ND in commissural and association fibers is in agreement with those of Rae et al, who described a widespread reduction in ND in a group of medicated first episode psychosis patients with an average illness duration of approximately two years (Rae et al., 2017), and reports of extensive reduced ND in a rat model of disrupted in

schizophrenia gene 1 (DISC-1; (Barnett et al., 2019)), a gene that is involved in regulation of cell proliferation, neuronal axon and dendrite outgrowth and implicated in the schizophrenia pathophysiology. However, our report of increased ND in the anterior thalamic radiation stands in in contrast with above findings. Interestingly, in this area, we also found excess FW which is often interpreted as evidence of inflammation (Kraguljac et al., 2019; Lyall et al., 2017; Oestreich et al., 2017; Oestreich et al., 2016). Increased ND in pathological states has been reported previously. For example, amyloidosis with inflammatory conditioning induced by interleukin 6 (IL-6) increases ND in mice (Colon-Perez et al., 2019). ND also increases with chronological age (Chang et al., 2015). Thus, results could be interpreted as a reflection of premature aging, possibly in context of an inflammatory process, which was previously reported in patients with schizophrenia (Tønnesen et al., 2020). Taken together, the variable expressions of ND alterations in commissural, association and projection fibers could be understood as evidence of tract-specific neuropathological effects, which is consistent with a recent discovery that white matter changes in schizophrenia involve dynamic interactions between neuropathological processes in a tract-specific manner (Cetin-Karayumak et al., 2019).

We found widespread ODI increase in FEP, observed regional patterns are in agreement with previously reported white matter deficits in schizophrenia (Kelly et al., 2017). Based on studies in transparent mouse brains (Sato et al., 2017) and microscopic mapping studies in postmortem human brains (Mollink et al., 2017), greater ODI can be interpreted as evidence of lesser fiber uniformity. Consistently, we previously reported increased ODI in the internal capsule in never-treated and currently unmedicated schizophrenia patients (Kraguljac et al., 2019), the lesser spatial extent of alterations in that study may be attributable to the use of a single-shell diffusion sequence which is less robust in quantifying microarchitecture. Even though another study in medicated first episode patients, cross-sectionally assessed at 1.5 tesla, did not find ODI abnormalities, they did report evidence of fiber geometry changes with increasing age in patients (Rae et al., 2017). Given the smaller sample size (35 patients, 19 controls), it is possible that they were slightly underpowered to detect ODI increases in patients.

Consistent with the literature (Lesh et al., 2019; Lyall et al., 2017; Oestreich et al., 2017; Oestreich et al., 2016), we found increased FW in the anterior corona radiata and the anterior thalamic radiation. Unexpectedly, we also detected decreased FW in the inferior longitudinal fasciculus and corticospinal tract in patients; this has not been previously reported in the schizophrenia literature. A recent mechanistic paper demonstrated that blood flow in the capillary bed may have an effect on the estimation of the free water fraction (Rydhog et al., 2017). Because mixed patterns of increased and decreased cerebral blood flow have previously been reported in schizophrenia (Pinkham et al., 2011), it is possible that the decrease in FW we noted in FEP may reflect altered cerebral blood flow in these regions. However, studies specifically designed to determine the contribution of blood flow alterations in pathological states on FW estimates need to be conducted before more definitive conclusions can be drawn.

It has been hypothesized that the prolonged development of associative white matter tracts may make these areas more vulnerable to the primary or secondary risk factors

of schizophrenia (Kochunov et al., 2016). The DUP has been identified as an important, potentially modifiable, secondary risk factor that adversely impacts clinical outcomes in the illness (Albert et al., 2017; Primavera et al., 2012). Here, we found that longer DUP was associated with greater white matter microarchitectural alterations across all NODDI indices, irrespective of fiber type. Spatial overlap between white matter alterations and associations between white matter integrity and DUP was evident in several white matter regions, including the superior longitudinal fasciculus, inferior fronto-occipital fasciculus, corpus callosum, arcuate fasciculus, internal capsule, anterior thalamic radiation. Greater DUP was associated with worse white matter integrity in the inferior fronto-occipital fasciculus which is a white matter structure that is associated with semantic processing deficits (Surbeck et al., 2020), thus offering a possible formal link between formal thought disorder and DUP on a neuroanatomical level. Interestingly, DUP also was associated with microarchitectural integrity in fiber tracts that were not yet considered abnormal when contrasting patients and controls. These fibers included the cingulum bundle and fornix (no ND abnormality, only a small area of ODI increase), which are two of the major white matter tracts in the limbic system (Abdul-Rahman et al., 2011). The limbic system was one of the earliest circuits implicated in the schizophrenia pathophysiology (Torrey and Peterson, 1974), but there is some debate as to whether this pathway plays a primary role in the genesis of schizophrenia or if abnormalities reflect a downstream process of the illness (White et al., 2008). Regardless, our data support the idea that DUP may adversely impact limbic microarchitecture, suggesting that early intervention could have the potential to attenuate limbic system pathology. It is important to note, that while DUP has been suggested as a marker of environmental effects in the pathogenesis of schizophrenia, based on our cross-sectional data it is not possible to definitively determine the directionality of the association. In other words, it remains unclear if DUP in fact has a causative role in NODDI alterations seen here, or if white matter pathology arisen during aberrant neurodevelopment drives some patients to have a more insidious course of the illness which is reflected by a longer DUP.

NODDI analyses showed significantly more widespread effects of DUP on white matter microarchitecture than would be expected based on our DTI findings in an overlapping patient sample (Kraguljac et al., 2020). This is in agreement with reports that advanced parameters may be more sensitive in detecting white matter disease signatures (Genc et al., 2017; Mah et al., 2017). In addition to providing more biologically informed specificity in quantification of microstructure, NODDI was shown to capture disease discriminative voxels that were not identified with standard DTI metrics in a head-to-head comparison (Timmers et al., 2016). Our results further underscore that is worthwhile to add model complexity and computational expense to data analytics pipelines in studies with a clinical population as it may detect disease signatures not captured by the standard DTI model.

An important strength of our study is that this cohort represents one the largest groups of psychosis spectrum patients recruited in neuroimaging studies at first treatment contact, even though this is a notoriously challenging population to recruit. This allowed us to mitigate confounds of antipsychotic medication exposure and illness chronicity. We determined DUP using a clinical interview which has shown to be no less reliable than standardized assessment tools (Register-Brown and Hong, 2014). Because DUP in our sample, as in many

other previous studies, was not normally distributed, we used a log transform to normalize data. Even though cannabis, a major risk factor developing psychosis, may affect brain structure (Cookey et al., 2014), we did not exclude patients with a history of cannabis use as this would have inadvertently biased our sample and limit the generalizability of our data. We used a human connectome style two-shell diffusion weighted imaging protocol for data acquisition. While parameters were not specifically optimized for NODDI, a head to head comparison of several acquisition protocols for the assessment of NODDI indices concluded that the relative performance of the protocol depends primarily on the number of sampled orientations (Zhang et al., 2012). Our sequence sampled 98 orientations for each sampling direction which is comparable to the number of directions used other NODDI diffusion sequences. It was further demonstrated that NODDI parameters can be reliably estimated using two-shell protocols, and found that the number of shells is not a key factor in the assessment of white matter NODDI parameters (Zhang et al., 2012), supporting that our sequence parameters were sufficient for this type of modeling. As with any type of imaging, subject motion is a confounding factor that affect data quality and is difficult to truly control for. We used a priori defined cutoff points for subject motion and included individual motion parameters in statistical analysis, but is possible that subtle differences in subject motion between groups may have affected findings.

5. CONCLUSIONS

In summary, we demonstrated that complex microarchitecture abnormalities are already evident in antipsychotic-naïve first episode psychosis patients. Spatial patterns suggest that ND alterations are differentially expressed depending on fiber type, while decreased fiber complexity appears to be a uniform marker of white matter deficits in the illness. Importantly, we identified an empirical link between longer DUP, a major environmental factor adversely affecting long term clinical outcomes, and greater white matter pathology across NODDI indices, underscoring the critical importance of early intervention in this devastating illness.

CONFLICT OF INTEREST

This work was supported by the National Institute of Mental Health (R01MH112800 and R01MH102951, ACL; K23MH106683, NVK). We would like to thank UAB IT Research Computing for providing the HPC resources (compute, storage and networking) for this project. Cheaha is supported in part by the National Science Foundation under Grant No. OAC-1541310, the University of Alabama at Birmingham, and the Alabama Innovation Fund.

Dr. Kraguljac serves as consultant for Neurocrine Biosciences, Inc. All other authors declare no conflicts of interest, including relevant financial interests, activities, relationships, and affiliations.

REFERENCES

Abdul-Rahman MF, Qiu A, Sim K, 2011. Regionally specific white matter disruptions of fornix and cingulum in schizophrenia. PLoS One 6, e18652. [PubMed: 21533181]

Albert N, Melau M, Jensen H, Hastrup LH, Hjorthoj C, Nordentoft M, 2017. The effect of duration of untreated psychosis and treatment delay on the outcomes of prolonged early intervention in psychotic disorders. NPJ Schizophr 3, 34. [PubMed: 28951544]

Assaf Y, Basser PJ, 2005. Composite hindered and restricted model of diffusion (CHARMED) MR imaging of the human brain. Neuroimage 27, 48–58. [PubMed: 15979342]

Barnett BR, Torres-Velazquez M, Yi SY, Rowley PA, Sawin EA, Rubinstein CD, Krentz K, Anderson JM, Bakshi VP, Yu JJ, 2019. Sex-specific deficits in neurite density and white matter integrity are associated with targeted disruption of exon 2 of the Disc1 gene in the rat. Transl Psychiatry 9, 82. [PubMed: 30745562]

Brouwer RM, Mandl RC, Schnack HG, van Soelen IL, van Baal GC, Peper JS, Kahn RS, Boomsma DI, Hulshoff Pol HE, 2012. White matter development in early puberty: a longitudinal volumetric and diffusion tensor imaging twin study. PLoS One 7, e32316. [PubMed: 22514599]

Carpenter WT Jr., Gold JM, Lahti AC, Queern CA, Conley RR, Bartko JJ, Kovnick J, Appelbaum PS, 2000. Decisional capacity for informed consent in schizophrenia research. Arch Gen Psychiatry 57, 533–538. [PubMed: 10839330]

Cetin-Karayumak S, Di Biase MA, Chunga N, Reid B, Somes N, Lyall AE, Kelly S, Solgun B, Pasternak O, Vangel M, Pearlson G, Tamminga C, Sweeney JA, Clementz B, Schretlen D, Viher PV, Stegmayer K, Walther S, Lee J, Crow T, James A, Voineskos A, Buchanan RW, Szeszko PR, Malhotra AK, Hegde R, McCarley R, Keshavan M, Shenton M, Rathi Y, Kubicki M, 2019. White matter abnormalities across the lifespan of schizophrenia: a harmonized multi-site diffusion MRI study. Mol Psychiatry.

Chang YS, Owen JP, Pojman NJ, Thieu T, Bukshpun P, Wakahiro ML, Berman JI, Roberts TP, Nagarajan SS, Sherr EH, Mukherjee P, 2015. White Matter Changes of Neurite Density and Fiber Orientation Dispersion during Human Brain Maturation. PLoS One 10, e0123656. [PubMed: 26115451]

Chiang MC, McMahon KL, de Zubicaray GI, Martin NG, Hickie I, Toga AW, Wright MJ, Thompson PM, 2011. Genetics of white matter development: a DTI study of 705 twins and their siblings aged 12 to 29. Neuroimage 54, 2308–2317. [PubMed: 20950689]

Colgan N, Siow B, O'Callaghan JM, Harrison IF, Wells JA, Holmes HE, Ismail O, Richardson S, Alexander DC, Collins EC, Fisher EM, Johnson R, Schwarz AJ, Ahmed Z, O'Neill MJ, Murray TK, Zhang H, Lythgoe MF, 2016. Application of neurite orientation dispersion and density imaging (NODDI) to a tau pathology model of Alzheimer's disease. Neuroimage 125, 739–744. [PubMed: 26505297]

Colon-Perez LM, Ibanez KR, Suarez M, Torroella K, Acuna K, Ofori E, Levites Y, Vaillancourt DE, Golde TE, Chakrabarty P, Febo M, 2019. Neurite orientation dispersion and density imaging reveals white matter and hippocampal microstructure changes produced by Interleukin-6 in the TgCRND8 mouse model of amyloidosis. Neuroimage 202, 116138. [PubMed: 31472250]

Cookey J, Bernier D, Tibbo PG, 2014. White matter changes in early phase schizophrenia and cannabis use: an update and systematic review of diffusion tensor imaging studies. Schizophr Res 156, 137–142. [PubMed: 24842540]

Cox RW, Chen G, Glen DR, Reynolds RC, Taylor PA, 2017. fMRI clustering and false-positive rates. Proc Natl Acad Sci U S A 114, E3370–E3371. [PubMed: 28420798]

Fick HJ, Daianu M, Pizzolato M, Wassermann D, Jacobs RE, Thompson PM, Town T, Deriche R, 2017. Comparison of biomarkers in transgenic alzheimer rats using multi-shell diffusio MRI. In: Fluster A, Gohosh A, Kaden E, Rathi Y, Reisert M (Eds.), computational Diffusio MRI. Springer, Chambridge.

Fieremans E, Jensen JH, Helpern JA, 2011. White matter characterization with diffusional kurtosis imaging. Neuroimage 58, 177–188. [PubMed: 21699989]

Genc S, Malpas CB, Holland SK, Beare R, Silk TJ, 2017. Neurite density index is sensitive to age related differences in the developing brain. Neuroimage 148, 373–380. [PubMed: 28087489]

Grussu F, Schneider T, Tur C, Yates RL, Tachrount M, Ianus A, Yiannakas MC, Newcombe J, Zhang H, Alexander DC, DeLuca GC, Gandini Wheeler-Kingshott CAM, 2017. Neurite dispersion: a new marker of multiple sclerosis spinal cord pathology? Ann Clin Transl Neurol 4, 663–679. [PubMed: 28904988]

Hasan KM, Kamali A, Iftikhar A, Kramer LA, Papanicolaou AC, Fletcher JM, Ewing-Cobbs L, 2009. Diffusion tensor tractography quantification of the human corpus callosum fiber pathways across the lifespan. Brain Res 1249, 91–100. [PubMed: 18996095]

Irfanoglu MO, Modi P, Nayak A, Hutchinson EB, Sarlls J, Pierpaoli C, 2015. DR-BUDDI (Diffeomorphic Registration for Blip-Up blip-Down Diffusion Imaging) method for correcting echo planar imaging distortions. Neuroimage 106, 284–299. [PubMed: 25433212]

Irfanoglu MO, Nayak A, Jenkins J, Pierpaoli C, 2017. TORTOISEv3:Improvements and new features of the NIH diffusion MRI processing pipeline. ISMRM 25th annual meeting, Honolulu, HI.

Kellner E, Dhital B, Kiselev VG, Reisert M, 2016. Gibbs-ringing artifact removal based on local subvoxel-shifts. Magn Reson Med 76, 1574–1581. [PubMed: 26745823]

Kelly S, Jahanshad N, Zalesky A, Kochunov P, Agartz I, Alloza C, Andreassen OA, Arango C, Banaj N, Bouix S, Bousman CA, Brouwer RM, Bruggemann J, Bustillo J, Cahn W, Calhoun V, Cannon D, Carr V, Catts S, Chen J, Chen JX, Chen X, Chiapponi C, Cho KK, Ciullo V, Corvin AS, Crespo-Facorro B, Cropley V, De Rossi P, Diaz-Caneja CM, Dickie EW, Ehrlich S, Fan FM, Faskowitz J, Fatouros-Bergman H, Flyckt L, Ford JM, Fouche JP, Fukunaga M, Gill M, Glahn DC, Gollub R, Goudzwaard ED, Guo H, Gur RE, Gur RC, Gurholt TP, Hashimoto R, Hatton SN, Henskens FA, Hibar DP, Hickie IB, Hong LE, Horacek J, Howells FM, Hulshoff Pol HE, Hyde CL, Isaev D, Jablensky A, Jansen PR, Janssen J, Jonsson EG, Jung LA, Kahn RS, Kikinis Z, Liu K, Klauser P, Knochel C, Kubicki M, Lagopoulos J, Langen C, Lawrie S, Lenroot RK, Lim KO, Lopez-Jaramillo C, Lyall A, Magnotta V, Mandl RCW, Mathalon DH, McCarley RW, McCarthy-Jones S, McDonald C, McEwen S, McIntosh A, Melicher T, Mesholam-Gately RI, Michie PT, Mowry B, Mueller BA, Newell DT, O'Donnell P, Oertel-Knochel V, Oestreich L, Paciga SA, Pantelis C, Pasternak O, Pearlson G, Pellicano GR, Pereira A, Pineda Zapata J, Piras F, Potkin SG, Preda A, Rasser PE, Roalf DR, Roiz R, Roos A, Rotenberg D, Satterthwaite TD, Savadjiev P, Schall U, Scott RJ, Seal ML, Seidman LJ, Shannon Weickert C, Whelan CD, Shenton ME, Kwon JS, Spalletta G, Spaniel F, Sprooten E, Stablein M, Stein DJ, Sundram S, Tan Y, Tan S, Tang S, Temmingh HS, Westlye LT, Tonnesen S, Tordesillas-Gutierrez D, Doan NT, Vaidya J, van Haren NEM, Vargas CD, Vecchio D, Velakoulis D, Voineskos A, Voyvodic JQ, Wang Z, Wan P, Wei D, Weickert TW, Whalley H, White T, Whitford TJ, Wojcik JD, Xiang H, Xie Z, Yamamori H, Yang F, Yao N, Zhang G, Zhao J, van Erp TGM, Turner J, Thompson PM, Donohoe G, 2017. Widespread white matter microstructural differences in schizophrenia across 4322 individuals: results from the ENIGMA Schizophrenia DTI Working Group. Mol Psychiatry.

Kelly S, Jahanshad N, Zalesky A, Kochunov P, Agartz I, Alloza C, Andreassen OA, Arango C, Banaj N, Bouix S, Bousman CA, Brouwer RM, Bruggemann J, Bustillo J, Cahn W, Calhoun V, Cannon D, Carr V, Catts S, Chen J, Chen JX, Chen X, Chiapponi C, Cho KK, Ciullo V, Corvin AS, Crespo-Facorro B, Cropley V, De Rossi P, Diaz-Caneja CM, Dickie EW, Ehrlich S, Fan FM, Faskowitz J, Fatouros-Bergman H, Flyckt L, Ford JM, Fouche JP, Fukunaga M, Gill M, Glahn DC, Gollub R, Goudzwaard ED, Guo H, Gur RE, Gur RC, Gurholt TP, Hashimoto R, Hatton SN, Henskens FA, Hibar DP, Hickie IB, Hong LE, Horacek J, Howells FM, Hulshoff Pol HE, Hyde CL, Isaev D, Jablensky A, Jansen PR, Janssen J, Jonsson EG, Jung LA, Kahn RS, Kikinis Z, Liu K, Klauser P, Knochel C, Kubicki M, Lagopoulos J, Langen C, Lawrie S, Lenroot RK, Lim KO, Lopez-Jaramillo C, Lyall A, Magnotta V, Mandl RCW, Mathalon DH, McCarley RW, McCarthy-Jones S, McDonald C, McEwen S, McIntosh A, Melicher T, Mesholam-Gately RI, Michie PT, Mowry B, Mueller BA, Newell DT, O'Donnell P, Oertel-Knochel V, Oestreich L, Paciga SA, Pantelis C, Pasternak O, Pearlson G, Pellicano GR, Pereira A, Pineda Zapata J, Piras F, Potkin SG, Preda A, Rasser PE, Roalf DR, Roiz R, Roos A, Rotenberg D, Satterthwaite TD, Savadjiev P, Schall U, Scott RJ, Seal ML, Seidman LJ, Shannon Weickert C, Whelan CD, Shenton ME, Kwon JS, Spalletta G, Spaniel F, Sprooten E, Stablein M, Stein DJ, Sundram S, Tan Y, Tan S, Tang S, Temmingh HS, Westlye LT, Tonnesen S, Tordesillas-Gutierrez D, Doan NT, Vaidya J, van Haren NEM, Vargas CD, Vecchio D, Velakoulis D, Voineskos A, Voyvodic JQ, Wang Z, Wan P, Wei D, Weickert TW, Whalley H, White T, Whitford TJ, Wojcik JD, Xiang H, Xie Z, Yamamori H, Yang F, Yao N, Zhang G, Zhao J, van Erp TGM, Turner J, Thompson PM, Donohoe G, 2018. Widespread white matter microstructural differences in schizophrenia across 4322 individuals: results from the ENIGMA Schizophrenia DTI Working Group. Mol Psychiatry 23, 1261–1269. [PubMed: 29038599]

Kochunov P, Ganjgahi H, Winkler A, Kelly S, Shukla DK, Du X, Jahanshad N, Rowland L, Sampath H, Patel B, O'Donnell P, Xie Z, Paciga SA, Schubert CR, Chen J, Zhang G, Thompson PM, Nichols TE, Hong LE, 2016. Heterochronicity of white matter development and aging explains regional patient control differences in schizophrenia. Hum Brain Mapp 37, 4673–4688. [PubMed: 27477775]

Kochunov P, Hong LE, 2014. Neurodevelopmental and neurodegenerative models of schizophrenia: white matter at the center stage. Schizophr Bull 40, 721–728. [PubMed: 24870447]

Kochunov P, Williamson DE, Lancaster J, Fox P, Cornell J, Blangero J, Glahn DC, 2012. Fractional anisotropy of water diffusion in cerebral white matter across the lifespan. Neurobiol Aging 33, 9–20. [PubMed: 20122755]

Kraguljac NV, Anthony T, Monroe WS, Skidmore FM, Morgan CJ, White DM, Patel N, Lahti AC, 2019. A longitudinal neurite and free water imaging study in patients with a schizophrenia spectrum disorder. Neuropsychopharmacology 44, 1932–1939. [PubMed: 31153156]

Kraguljac NV, Anthony T, Morgan CJ, Jindal RD, Burger MS, Lahti AC, 2020. White matter integrity, duration of untreated psychosis, and antipsychotic treatment response in medication-naive first-episode psychosis patients. Mol Psychiatry.

Lebel C, Deoni S, 2018. The development of brain white matter microstructure. Neuroimage 182, 207–218. [PubMed: 29305910]

Lesh TA, Maddock RJ, Howell A, Wang H, Tanase C, Daniel Ragland J, Niendam TA, Carter CS, 2019. Extracellular free water and glutathione in first-episode psychosis-a multimodal investigation of an inflammatory model for psychosis. Mol Psychiatry.

Lyall AE, Pasternak O, Robinson DG, Newell D, Trampush JW, Gallego JA, Fava M, Malhotra AK, Karlsgodt KH, Kubicki M, Szeszko PR, 2017. Greater extracellular free-water in first-episode psychosis predicts better neurocognitive functioning. Mol Psychiatry.

Mah A, Geeraert B, Lebel C, 2017. Detailing neuroanatomical development in late childhood and early adolescence using NODDI. PLoS One 12, e0182340. [PubMed: 28817577]

Mollink J, Kleinnijenhuis M, Cappellen van Walsum AV, Sotiropoulos SN, Cottaar M, Mirfin C, Heinrich MP, Jenkinson M, Pallebage-Gamarallage M, Ansorge O, Jbabdi S, Miller KL, 2017. Evaluating fibre orientation dispersion in white matter: Comparison of diffusion MRI, histology and polarized light imaging. Neuroimage 157, 561–574. [PubMed: 28602815]

Oestreich LK, Lyall AE, Pasternak O, Kikinis Z, Newell DT, Savadjiev P, Bouix S, Shenton ME, Kubicki M, Australian Schizophrenia Research B, Whitford TJ, McCarthy-Jones S, 2017. Characterizing white matter changes in chronic schizophrenia: A free-water imaging multi-site study. Schizophr Res.

Oestreich LK, Pasternak O, Shenton ME, Kubicki M, Gong X, Australian Schizophrenia Research B, McCarthy-Jones S, Whitford TJ, 2016. Abnormal white matter microstructure and increased extracellular free-water in the cingulum bundle associated with delusions in chronic schizophrenia. Neuroimage Clin 12, 405–414. [PubMed: 27622137]

Ozarslan E, Koay CG, Shepherd TM, Komlosh ME, Irfanoglu MO, Pierpaoli C, Basser PJ, 2013. Mean apparent propagator (MAP) MRI: a novel diffusion imaging method for mapping tissue microstructure. Neuroimage 78, 16–32. [PubMed: 23587694]

Pierpaoli C, Walker L, Irfanoglu MO, Barnett A, Basser P, Chang L-C, Koay C, Pajevic S, Rohde G, Sarlls J, Wu M, 2010. TORTOISE: an integrated software package for processing of diffusion MRI data. ISMRM 18th annual meeting, Stockholm, Sweden.

Pinkham A, Loughead J, Ruparel K, Wu WC, Overton E, Gur R, Gur R, 2011. Resting quantitative cerebral blood flow in schizophrenia measured by pulsed arterial spin labeling perfusion MRI. Psychiatry Res 194, 64–72. [PubMed: 21831608]

Primavera D, Bandecchi C, Lepori T, Sanna L, Nicotra E, Carpiniello B, 2012. Does duration of untreated psychosis predict very long term outcome of schizophrenic disorders? results of a retrospective study. Ann Gen Psychiatry 11, 21. [PubMed: 22856624]

Rae CL, Davies G, Garfinkel SN, Gabel MC, Dowell NG, Cercignani M, Seth AK, Greenwood KE, Medford N, Critchley HD, 2017. Deficits in Neurite Density Underlie White Matter Structure Abnormalities in First-Episode Psychosis. Biol Psychiatry 82, 716–725. [PubMed: 28359565]

Register-Brown K, Hong LE, 2014. Reliability and validity of methods for measuring the duration of untreated psychosis: a quantitative review and meta-analysis. Schizophr Res 160, 20–26. [PubMed: 25464915]

Rohde GK, Barnett AS, Basser PJ, Marenco S, Pierpaoli C, 2004. Comprehensive approach for correction of motion and distortion in diffusion-weighted MRI. Magn Reson Med 51, 103–114. [PubMed: 14705050]

Rydhog AS, Szczepankiewicz F, Wirestam R, Ahlgren A, Westin CF, Knutsson L, Pasternak O, 2017. Separating blood and water: Perfusion and free water elimination from diffusion MRI in the human brain. Neuroimage 156, 423–434. [PubMed: 28412443]

Sato K, Kerever A, Kamagata K, Tsuruta K, Irie R, Tagawa K, Okazawa H, Arikawa-Hirasawa E, Nitta N, Aoki I, Aoki S, 2017. Understanding microstructure of the brain by comparison of neurite orientation dispersion and density imaging (NODDI) with transparent mouse brain. Acta Radiol Open 6, 2058460117703816.

Schilling KG, Janve V, Gao Y, Stepniewska I, Landman BA, Anderson AW, 2018. Histological validation of diffusion MRI fiber orientation distributions and dispersion. Neuroimage 165, 200–221. [PubMed: 29074279]

Surbeck W, Hanggi J, Scholtes F, Viher PV, Schmidt A, Stegmayer K, Studerus E, Lang UE, Riecher-Rossler A, Strik W, Seifritz E, Borgwardt S, Quednow BB, Walther S, 2020. Anatomical integrity within the inferior fronto-occipital fasciculus and semantic processing deficits in schizophrenia spectrum disorders. Schizophr Res 218, 267–275. [PubMed: 31948896]

Sykova E, Nicholson C, 2008. Diffusion in brain extracellular space. Physiol Rev 88, 1277–1340. [PubMed: 18923183]

Timmers I, Roebroeck A, Bastiani M, Jansma B, Rubio-Gozalbo E, Zhang H, 2016. Assessing Microstructural Substrates of White Matter Abnormalities: A Comparative Study Using DTI and NODDI. PLoS One 11, e0167884. [PubMed: 28002426]

Tønnesen S, Kaufmann T, de Lange A-M, Richard G, Doan NT, Alnæs D, van der Meer D, Rokicki J, Moberget T, Maximov II, Agartz I, Aminoff SR, Beck D, Barch D, Beresniewicz J, Cervenka S, Bergman HF, Craven AR, Flyckt L, Gurholt TP, Haukvik UK, Hugdahl K, Johnsen E, Jönsson EG, Kolskår KK, Kompus K, Kroken RA, Lagerberg TV, Løberg E-M, Nordvik JE, Sanders A-M, Ulrichsen K, Andreassen OA, Westlye LT, 2020. Brain age prediction reveals aberrant brain white matter in schizophrenia and bipolar disorder: A multi-sample diffusion tensor imaging study. bioRxiv, 607754.

Torrey EF, Peterson MR, 1974. Schizophrenia and the limbic system. Lancet 2, 942–946. [PubMed: 4138925]

Veraart J, Fieremans E, Novikov DS, 2016. Diffusion MRI noise mapping using random matrix theory. Magn Reson Med 76, 1582–1593. [PubMed: 26599599]

White T, Cullen K, Rohrer LM, Karatekin C, Luciana M, Schmidt M, Hongwanishkul D, Kumra S, Charles Schulz S, Lim KO, 2008. Limbic structures and networks in children and adolescents with schizophrenia. Schizophr Bull 34, 18–29. [PubMed: 17942479]

Yin J, Liu Y, Crosby LD, Anthony T, Burdyshaw C, Brook RG, Marstrander J, Horton M, Skidmore FM, 2016. Optimization of non-linear image registration in AFNI. XSEDE. ACM, Miami, Florida.

Zhang H, Schneider T, Wheeler-Kingshott CA, Alexander DC, 2012. NODDI: practical in vivo neurite orientation dispersion and density imaging of the human brain. Neuroimage 61, 1000–1016. [PubMed: 22484410]

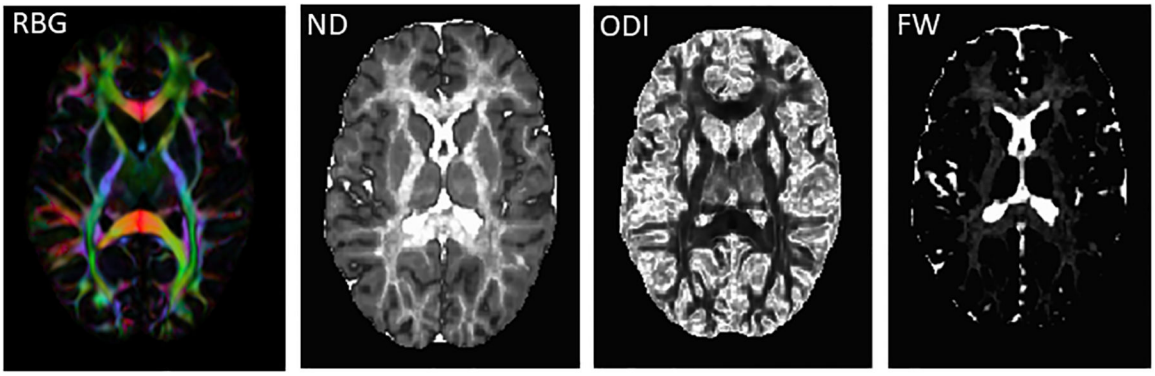

Figure 1:
Neurite Orientation Dispersion and Density Imaging (NODDI) maps. Abbreviations: RGB: red-green-blue color map indicating eigenvector orientations. ND: neurite density map, ODI: orientation dispersion index map, FW: extracellular free water map.

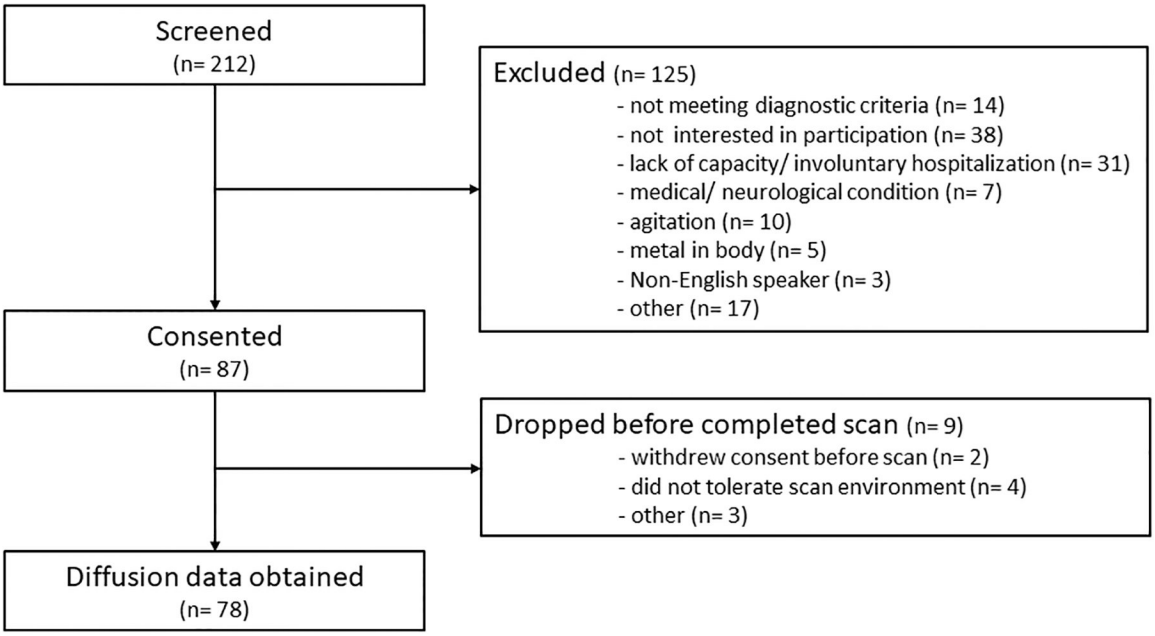

Figure 2:
CONSORT flow chart

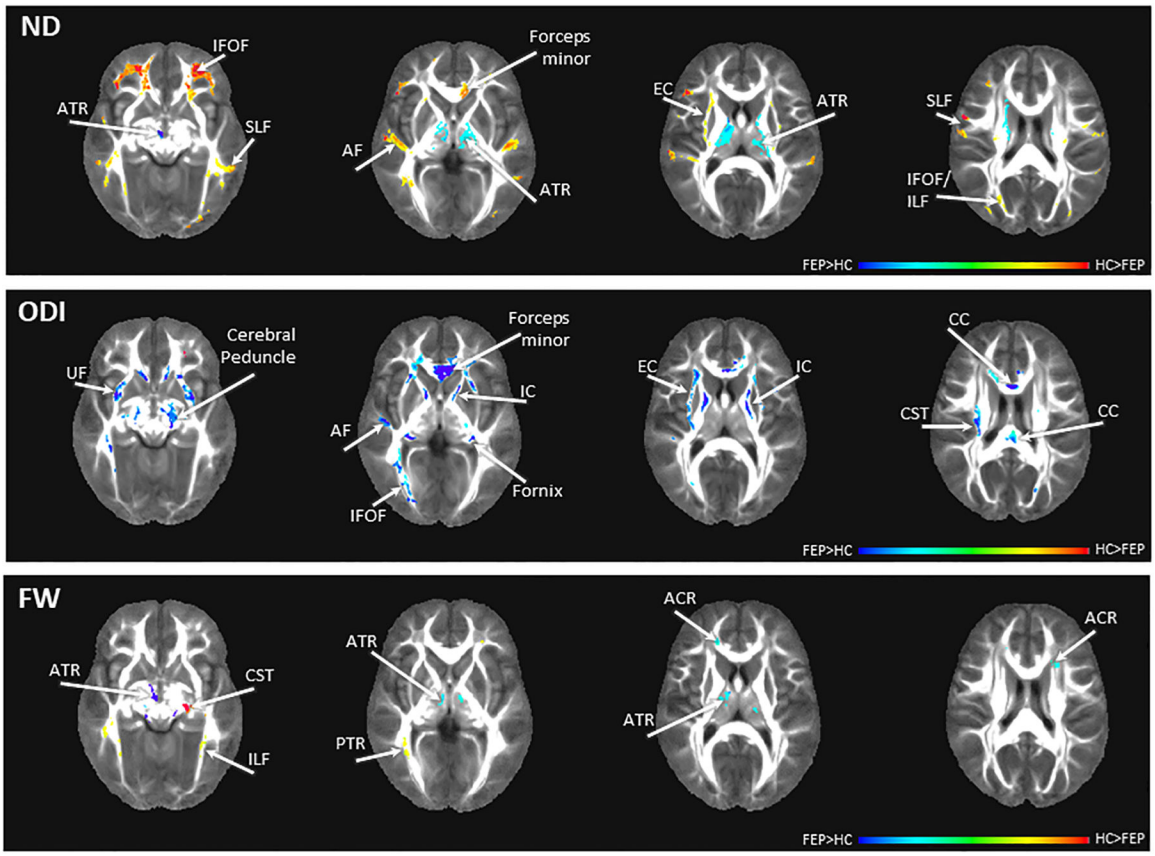

Figure 3:

Group differences in NODDI maps between first episode psychosis patients (FEP) and healthy controls (HC). Red scale colors indicate values are higher in HC, blue scale colors indicate values are higher in FEP. Abbreviations: ND: neurite density map, ODI: orientation dispersion index map, FW: extracellular free water map, ACR: anterior corona radiata, AF: arcuate fasciculus, ATR: anterior thalamic radiation, CC: corpus callosum, CST: corticospinal tract, EC: external capsule, IC: internal capsule, IFOF: inferior fronto-occipital fasciculus, ILF: inferior longitudinal fasciculus, PTR: posterior thalamic radiation, SLF: superior longitudinal fasciculus, UF: uncinate fasciculus. The color bar refers to z scores (for illustrative purposes a range from −0.4 to 0.4 was chosen). Blue/teal color range depicts areas of significantly higher diffusion values in patients compared to controls, yellow/red color range depicts areas of significantly lower diffusion values in patients compared to controls.

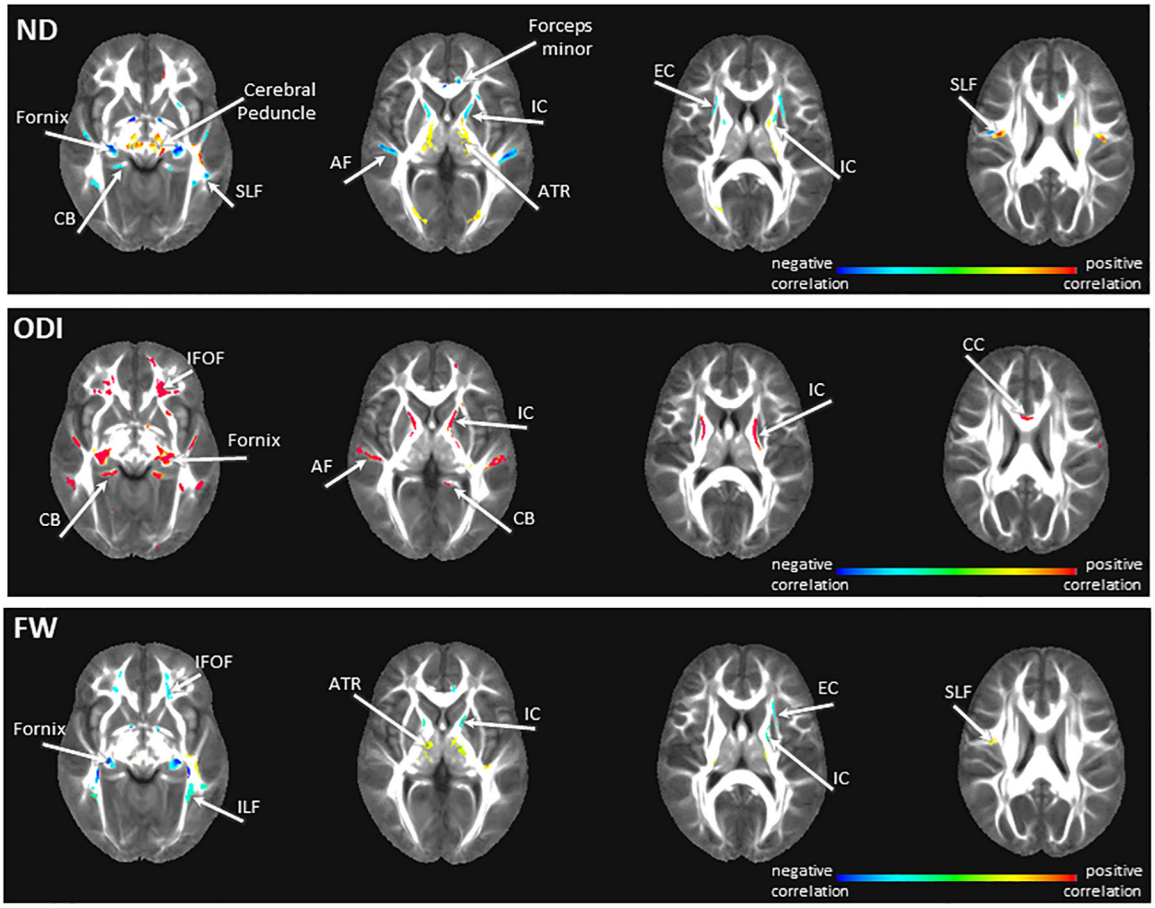

Figure 4:

Relationships between NODDI maps and duration of untreated psychosis (DUP) in first episode psychosis patients. Red scale colors indicate a positive correlation between DUP and NODDI indices, blue scale colors indicate a negative relationship between DUP and NODDI indices. Abbreviations: ND: neurite density map, ODI: orientation dispersion index map, FW: extracellular free water map, AF: arcuate fasciculus, ATR: anterior thalamic radiation, CB: cingulum bundle, CC: corpus callosum, EC: externa capsule, IFOF: inferior fronto-occipital fasciculus, ILF: inferior longitudinal fasciculus IC: internal capsule, SLF: superior longitudinal fasciculus. The color bar refers to z scores (for illustrative purposes a range from −0.4 to 0.4 was chosen). Blue/teal color range depicts areas of significant negative correlations between diffusion values and DUP, yellow/red color range depicts areas of significant positive correlations between diffusion values and DUP.

Table:

Demographics, clinical measures, and motion parameters[a]

	FEP (n= 78)	HC (n= 64)	t/X²/F	p value
Demographic variables				
Gender (% male)	64.1	64.1	0.00	1.0
Age	23.71 (5.96)	24.27 (5.87)	0.56	.58
Parental Occupation[b]	5.46 (4.62)	4.23 (3.99)	16.27	.43
Clinical variables				
Diagnosis				
Schizophrenia	41			
Schizoaffective Disorder	15			
Schizophreniform Disorder	3			
Brief Psychotic Disorder	2			
Bipolar Disorder with psychosis	3			
Major Depression with psychosis	2			
Unspecified Psychosis	12			
Duration of untreated psychosis [in months; median, mean, (SD)][c]	7; 23.50 (40.59)			
UDS +cannabis (%)	32.1			
BPRS[d]				
Total	49.75 (11.47)			
Positive	15.62 (4.10)			
Negative	5.71 (3.10)			
RBANS[e]				
Total index	73.49 (15.21)	92.47 (10.96)	8.11	< .01
Immediate memory	80.94 (16.68)	101.05 (15.99)	6.87	< .01
Visuospatial	74.25 (11.62)	82.33 (13.02)	2.95	< .01
Language	80.94 (16.68)	97.50 (14.91)	4.84	< .01
Attention span	79.81 (16.72)	101.57 (15.95)	7.43	< .01
Delayed memory	76.25 (15.69)	90.98 (8.78)	6.62	< .01
Scan quality data				
DWI[f]				
RMS absolute motion (mm)	0.39 (0.24)	0.32 (0.20)	−1.90	.06
RMS relative motion (mm)	0.007 (0.006)	0.005 (0.004)	−1.62	.10

FEP, first episode psychosis patient; HC, healthy control; UDS, urine drug screen; DWI, diffusion weighted image; DWI, diffusion weighted imaging; RMS, root mean square of the six motion parameters (translations and rotations)

[a]Mean (SD) unless indicated otherwise

[b]Ranks determined from Diagnostic Interview for Genetic Studies (1 – 18 scale); higher rank (lower numerical value) corresponds to higher socioeconomic status

[c]data not available for one subject

[d] Brief Psychiatric Rating Scale (1 – 7 scale); positive (conceptual disorganization, hallucinatory behavior, suspiciousness and unusual thought content); negative (emotional withdrawal, motor retardation, and blunted affect); data available for 77 patients

[e] Repeatable Battery for the Assessment of Neuropsychological Status; data available for 58 HC and 68 FEP

[f] data available for 59 HC and 61 FEP